Biosensors and Bioelectronics xx (xxxx) xxxx–xxxx

Contents lists available at ScienceDirect

Biosensors and Bioelectronics

journal homepage: www.elsevier.com/locate/bios

A fully integrated electrochemical biosensor platform fabrication process for cytokines detection

Abdoullatif Baraket[a], Michael Lee[a], Nadia Zine[a], Monique Sigaud[a], Joan Bausells[b], Abdelhamid Errachid[a,*]

[a] Université de Lyon, Institut des Sciences Analytiques, UMR 5280, CNRS, Université Lyon 1, ENS Lyon –5, rue de la Doua, F-69100 Villeurbanne, France
[b] Centro Nacional de Microelectrónica (IMB-CSIC) Campus UAB, Bellaterra, 08193 Barcelona, Spain

ARTICLE INFO

Keywords:
Biosensor platform
Cytokines
Electrochemical impedance spectroscopy
Multi-detection
Heart failure

ABSTRACT

Interleukin-1b (IL-1b) and interleukin-10 (IL-10) biomarkers are one of many antigens that are secreted in acute stages of inflammation after left ventricle assisted device (LVAD) implantation for patients suffering from heart failure (HF). In the present study, we have developed a fully integrated electrochemical biosensor platform for cytokine detection at minute concentrations. Using eight gold working microelectrodes (WEs) the design will increase the sensitivity of detection, decrease the time of measurements, and allow a simultaneous detection of varying cytokine biomarkers. The biosensor platform was fabricated onto silicon substrates using silicon technology. Monoclonal antibodies (mAb) of anti-human IL-1b and anti-human IL-10 were electroaddressed onto the gold WEs through functionalization with 4-carboxymethyl aryl diazonium (CMA). Cyclic voltammetry (CV) was applied during the WE functionalization process to characterize the gold WE surface properties. Finally, electrochemical impedance spectroscopy (EIS) characterized the modified gold WE. The biosensor platform was highly sensitive to the corresponding cytokines and no interference with other cytokines was observed. Both cytokines: IL-10 and IL-1b were detected within the range of 1 pg mL^{-1} to 15 pg mL^{-1}. The present electrochemical biosensor platform is very promising for multi-detection of biomolecules which can dramatically decrease the time of analysis. This can provide data to clinicians and doctors concerning cytokines secretion at minute concentrations and the prediction of the first signs of inflammation after LVAD implantation.

1. Introduction

Heart failure (HF), often called congestive heart failure (CHF) or congestive cardiac failure (CCF) occurs when the heart is unable to provide sufficient pump action to maintain blood flow to meet the needs of the body (Gullestad et al., 2012; Nymo et al., 2014; Slaughter et al., 2010). HF can cause a number of symptoms including shortness of breath, leg swelling, and exercise intolerance. Facing the difficulty of obtaining a sufficient number of donor organs, several bioelectronic devices such as pressure sensors and left ventricle assisted devices (LVADs) (Rohde et al., 2013) have been implanted into the patients' body in order to help the patient's heart and facilitate the continuation of patients' life until such a donor becomes available. The problem of organ biocompatibility as a direct cause to implanted LVADs can trigger increased pro- and anti-inflammatory cytokine levels (IL-10, IL-1, IL8, TNF-a, etc.) (Caruso et al., 2010; Kaptoge et al., 2014). This is amongst the principle origins of HF detection. Prior to LVAD implantation, Stumpf et al. (Stumpf et al., 2003) have reported on IL-10 plasma cytokine levels for 50 HF patients at 2.3 ± 1.9 pg mL^{-1}, while controls were measured at 5.2 ± 2.3 pg mL^{-1} ($P < 0.01$). In the same principle, Caruso et al. (Caruso et al., 2010) have reported on an exhaustive study for cytokines detection within survivors and non-survivors of 23 LVAD implanted patients. The collected data quantified exactly when patients were prone to higher levels of inflammation after cardiac surgery. Here, the authors have shown an early expression of human IL-10 and IL-1 peaked after LVAD implantation, when compared with other plasma samples analyzed within the 30 day period for survivors and non-survivors.

The standard technique for the detection of cardiac cytokines is based upon enzyme-linked immunosorbent assay (ELISA) (Navarri et al., 2015; Soman et al., 2011). Although this technique is highly sensitive and accurate, it is still time-consuming, requires specialized personnel, and requires at least 5 mL of sample for analysis. To overcome these problems, a highly sensitive biosensor and bio lab-on-chip were developed for the detection of the specific biomolecules (Benlarbi et al., 2012; Mazher-Iqbal and Desmulliez, 2011; Pui et al.,

* Corresponding author.
E-mail address: abdelhamid.errachid-el-salhi@univ-lyon1.fr (A. Errachid).

http://dx.doi.org/10.1016/j.bios.2016.09.023
Received 17 June 2016; Received in revised form 1 September 2016; Accepted 6 September 2016
Available online xxxx
0956-5663/

2011). These biosensors provide fast, real-time, and reliable medical diagnosis. This in turn, enhances the biomarkers detection at minute concentrations, thus, allowing the prediction of the first signs of inflammation. Several analytical analyses and techniques have been investigated for each developed biosensor, for e.g., optical, electromechanical, and electrochemical biosensors (Qureshi et al., 2012). These latter are widely reported as almost 50% of the biosensors used in the literature are based on electrochemical transducers (Dorothee et al., 2008; Kongsuphol et al., 2014). Previously, we have reported on electrochemical biosensors for TNF-α cytokine detection (Baraket et al., 2011). Here, the analyses were made by electrochemical impedance spectroscopy (EIS) onto a biocompatible and flexible material. This electrochemical technique is considered extremely sensitive to the weak variation changes that occur on the biosensor's surface. In the same principle, we have also reported on the detection of IL-10 by EIS using a new material substrate within complementary metal oxide semi-conductor (CMOS) technology (Lee et al., 2012). Here, the detection limit of IL-10 was 0.1 pg mL^{-1}. This can provide to clinicians, the first signs of cytokine secretion after LVAD transplantation.

The biofunctionalization of biosensors used mostly in the literature are based on self-assembled monolayers (SAMs) or cross-link to immobilize bioreceptors (Baraket et al., 2011; Baraket et al., 2016; Chebil et al., 2010; Hou et al., 2006; Prats-Alfonso et al., 2006). Although these techniques are highly adequate to support different techniques of detection, they remain limited by non-selectivity during biofunctionalization of an array of electrodes, for e.g., dropping the device in thiolated capture probe solution where thiol is adsorbed onto all working electrodes (WEs). To overcome this problem, an alternative technique was used in the literature to locally biofunctionalize microelectrodes. This is very important for multi-detection using several WEs in the same device (B. P. Corgier et al., 2005; Baraket et al., 2013; Corgier et al., 2007; Polsky et al., 2008).

In the present work, we report on the production of an electrochemical biosensor platform for multiple cytokine detection. This biosensor platform contains eight gold WEs allowing simultaneous and multiplex detection of different cytokines through electrically addressable diazonium-functionalized monoclonal antibodies (mAb's). Furthermore, this biosensor platform contains an integrated silver/silver chloride (Ag/AgCl) reference microelectrode (RE) and a platinum counter microelectrode (CE). The WEs, RE, and CE were fabricated onto a silicon substrate using silicon technology. Cyclic voltammetry (CV) was applied during the microelectrode functionalization process to confirm the mAb's immobilization and to characterize the gold microelectrodes surface properties. Finally, EIS characterization was applied onto the gold WEs for human IL-10 and IL-1b detection by the corresponding immobilized mAb, respectively.

2. Experimental

2.1. Reagents

4-carboxymethyl aryldiazonium(CMA), sodium nitrite ($NaNO_2$), hydrochloricacid (HCl) 37%, isopropyl alcohol (IPA) 96%, potassium chloride (KCl), N-hydroxysuccinimide (NHS), N-(3-dimethylaminopropyl)-N′-ethyl-carbodiimide hydrochloride (EDC), potassium ferrocyanide(II), potassium ferricyanide(III), and phosphate buffered saline (PBS) were purchased from *Sigma–Aldrich*, France. The immunoreagents: interleukin-10 (IL-10), interlukin-6 (IL-6), interleukin-1b (IL-1b) and mAb mouse anti-human IL-10/IL-6/IL-1b were purchased from *R & D Systems*, France.

2.2. Antibodies and cytokine preparation

Antibodies and cytokines were diluted in PBS buffer, aliquoted, and stored at −20 °C following the protocol of the supplier. The cytokines; IL-1, IL-6, and IL-10 were aliquoted before EIS measurements at different concentrations from 1, 5, 10, and 15 pg mL^{-1} respectively. These were stored at 4 °C. The antibodies; anti-IL-10 and anti-IL-1b were aliquoted at 10 mg mL^{-1}.

2.3. Instrumentation

The electrochemical experiments were carried out with a VMP3 multichannel potentiostat (Biologic-EC-Lab, France). CV technique was applied for diazonium-modified mAb deposition and EIS measurements were made to study the sensitivity and selectivity. All experiments were measured at room temperature. The modeling of the obtained EIS data was achieved by the EC-Lab software using the Randomize + Simplex method. Here, randomize was stopped on 100,000 iterations and the fit stopped on 5000 iterations.

2.4. Microelectronics technology

The devices were fabricated on 100 mm diameter silicon wafers. The metallic microelectrodes are isolated from the silicon substrate by a dielectric SiO_2 layer. It has a thickness of 800 nm and was grown by wet thermal oxidation. To fabricate the gold microelectrodes, a tri-layer of Ti (100 nm), Ni (150 nm), and Au (50 nm) was deposited by physical vapor deposition (PVD). The Ti layer ensures good adhesion to the SiO_2 and the Ni layer avoids intermixing of the Ti and Au. The microelectrode geometry was defined by photolithography and wet chemical etching. Next, the platinum microelectrodes were fabricated by PVD deposition of a metal bilayer of Ti (15 nm) plus Pt (150 nm), which was patterned by photolithography and a lift-off process. This was followed by the deposition of a dielectric passivation layer, obtained by plasma-enhanced chemical vapor deposition (PECVD) of SiO_2 (400 nm) plus Si_3N_4 (400 nm). The passivation layer was eliminated from the microelectrode areas and the contact pads by photolithography and dry reactive ion etching. Finally, silver for the reference electrodes was deposited by PVD as a bilayer of Ti (15 nm) plus Ag (150 nm) and patterned by photolithography plus lift-off. Fig. 1 shows the final image of the developed microelectrodes. Here, the chip integrates eight WEs in gold against a platinum CE and a silver RE.

Fig. 1(a) shows a topographic image of the chip taken by an optical 3D profilometer. The gold microelectrodes are detailed with a good definition. Measurements of electrical conduction showed the qualities of the metals deposited. The qualities of these metals play an important role in the process of chemical surface treatment and biofunctionalization of the chip after production.

The wafer was diced and the devices were glued to a printed circuit board (PCB) using an epoxy resin (Epo-Tek $H^{70}E-^{2}LC$, from *Epoxy Technology*) (Fig. 1b). Afterwards, the microelectrode pads were connected to the PCB board through aluminum wire (25 μm Ø) by wire-bonding (Kulicke & Soffa 4523 A) (Fig. 1c). Finally, the bonding area of the device, the bonding wires, and the gold tracks of the PCB were encapsulated using the same resin (Epo-Tek $H^{70}E-^{2}LC$) to protect them from the buffer or electrolyte solution (Fig. 1d). This resin is totally inert for any chemical reaction with buffers, electrolyte solution or other solvents, for e.g., acetone and ethanol.

2.5. Diazonium-antibody immobilization onto gold WEs

Before the electroaddressing of the CMA-modified mAb, the chip surface was cleaned with ethanol in an ultrasonic bath for 10 min and dried under nitrogen flow. The device was then placed under UV/O_3 for 20 min in order to remove all organic contaminants. After the cleaning procedure, the chip was incubated in 20 mg mL^{-1} of CMA-modified mAb's solution. Therefore, carboxyl diazonium (CMA) was previously covalently attached to the mAb's (Fig. 2(step1)) by EDC/NHS cross-linking with both at 0.1 M following the protocol used by P. Corgier et al. (B. P. Corgier et al., 2005). The CMA coupled to the mAb's was

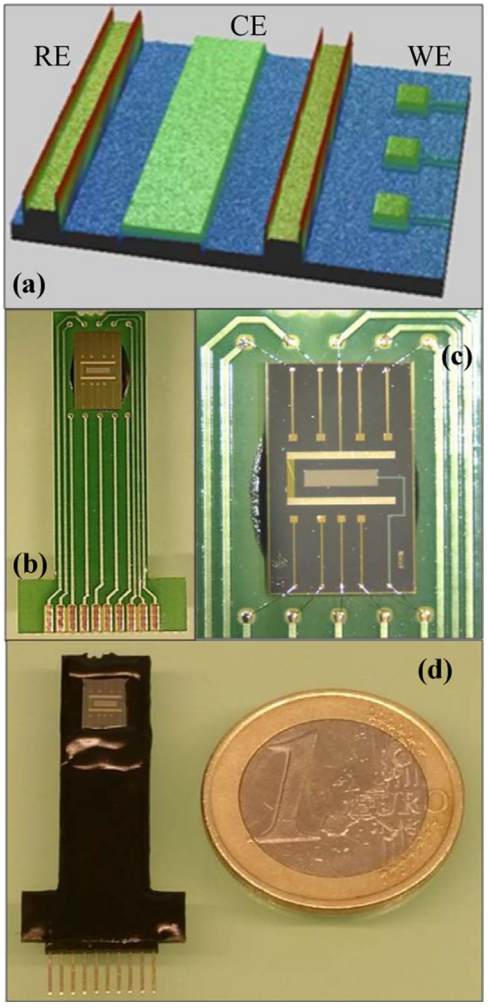

Fig. 1. (a) Interferometric topographic image of the chip fabricated on silicon showing the integrated reference electrode (RE), counter electrode (CE), and gold working microelectrodes (WEs), (b) optical image of the fixation of the biosensor platform onto the PCB board, (c) electrical connection of the microelectrode pads to the PCB board using wire bonding technique, and (d) the final biosensor platform after a total passivation with the epoxy resin.

then diazotated in an aqueous solution of HCl (20 mM) and $NaNO_2$ (20 mM) for 10 min (Fig. 2(step2)). Finally, and in order to locally biofunctionalize separate WEs, a five repetitive cyclic voltammogram was applied from 0.3 V to −1.4 V with a scan rate of 0.1 V/s onto the connected WEs (Fig. 2(step 3)). This was done sequentially until all desired microelectrodes were modified with the desired mAb (CMA-Anti-IL-10 and CMA-Anti-IL-1, respectively).

2.6. Cytokines detection by EIS measurements

EIS measurements were used to evaluate the recognition properties of the biosensor, in terms of sensitivity and selectivity. The measurement setup consisted of a biosensor platform where eight gold microelectrodes (225 μm^2) were used as WEs, a platinum CE (1980×480 µm) integrated in the same chip, and an external RE based on silver/silver chloride (Ag/AgCl) sizing 2908×180 µm from each side.

The impedance analysis was performed over a range of frequencies from 100 mHz to 100 kHz, using a modulation voltage of 25 mV. During the measurements, the potential was kept at 0.228 V versus an Ag/AgCl reference. Data acquisition and analysis were accomplished using EC-Lab software (Bio-Logic SAS, France).

The biosensor platform was applied to detect at the same time; human IL-10 and IL-1b cytokines within the concentration range of 1 pg mL^{-1} to 15 pg mL^{-1}. This range was chosen empirically, based on the interest for meeting both current needs in IL-10 and IL-1b sensitivity and establishing the lower detection limit. Therefore, CMA-mAb-IL-10 and CMA-mAb-IL-1b were immobilized onto two gold microelectrodes on the same biosensor platform. For analyte testing, the biosensor platform was subjected to successive incubations in the presence of different concentrations of human IL-10 and IL-1b solutions, for 30 min at 4 °C, followed by PBS washing. The impedance response was recorded for each concentration by immersing the biosensors in an electron mediator solution of 5 mM of $K_3[Fe(CN)_6]$/$K_4[Fe(CN)_6]$ in PBS buffer at pH 7.4.

3. Results

3.1. Chlorination of the integrated reference electrode

Before starting biofunctionalization of the biosensor and the detection process, the integrated RE based on silver material was chlorinated in order to have stable electrochemical analysis. Therefore, a chronoamperometric technique was used by applying a negative potential of −1.8 V during 1 min onto the integrated RE which was used as the WE. The chlorination process of the integrated RE was carried out with an external Ag/AgCl RE and with the integrated platinum CE. For chlorination, the electrolyte solution was prepared using 3 M potassium chloride dissolved in water.

Afterwards, the biosensor was washed with water, dried and used for electrochemical measurements using the all integrated Ag/AgCl RE and CE. Therefore, CV measurement was applied onto one gold WE of the biosensor, before and after chlorination of the RE (Fig. 3). CV measurements were performed in a solution of 5 mM of $K_3[Fe(CN)_6]$/$K_4[Fe(CN)_6]$ in PBS buffer at pH7.4. Before the chlorination process, the CV analyses drifted with increasing number of cycles as the integrated RE was based only on silver material. After the chlorination process, the same number of CV cycles was applied onto the same gold WE using the all integrated Ag/AgCl RE and CE. Here, all cycles were superimposed showing, thus the stable electrochemical analyses. The

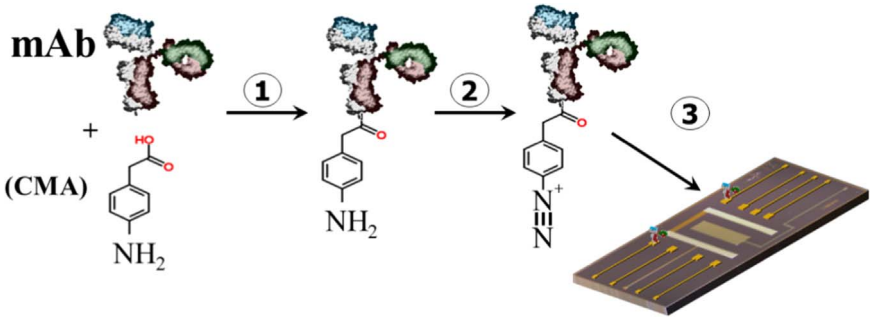

Fig. 2. Schematic illustration of CMA-mAb modification: (1) carboxyl diazonium was covalently attached to the mAb by EDC/NHS cross linking. (2) diazotation of CMA in an aqueous solution of HCl (20 mM) and $NaNO_2$ (20 mM) for 10 min (3) electroaddressing of CMA-modified mAb to the connected gold microelectrodes by applying five cycles of CV.

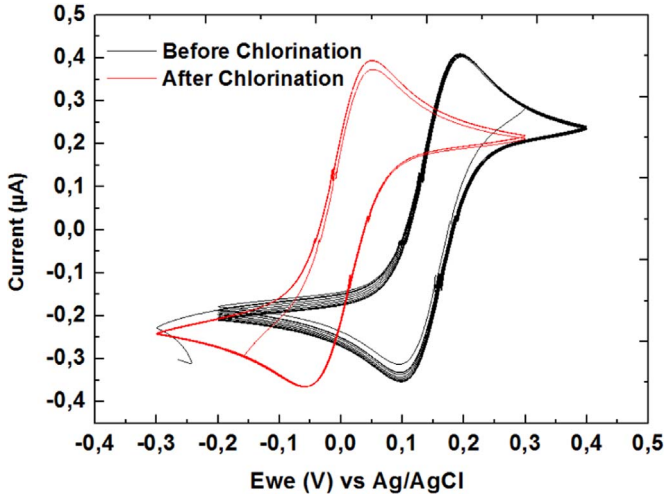

Fig. 3. Cyclic voltammetry (CV) of one working microelectrode (WE) of the biosensor platform, before and after chlorination of the RE using the all integrated reference and counter electrodes. CV measurement were performed in solution of 5 mM of $K_3[Fe(CN)_6]/K_4[Fe(CN)_6]$ in PBS buffer at pH7.4.

two CV analyses, before and after chlorination, were shifted due to the change of material surface for the RE and thus the change in potential between WE and RE.

3.2. Diazonium-antibody immobilization onto gold WEs

The CV of electroaddressing is shown in Fig. 4(I). The initial cycle in Fig. 4(I) shows a broad and irreversible cathodic wave with a peak potential at −1 V that indicates diazotated CMA-modified anti-IL-10 attachment onto the gold microelectrode surface by diazonium salt reduction. However, no reduction wave was observed upon deposition of the CMA-modified anti-IL-10. The immobilization of the latter was also confirmed by a variation of the CV before and after gold microelectrodes modification (Fig. 4(II)). Here, an important decrease in peak-to-peak of the CV cycle was observed when compared to the bare gold microelectrodes. This was attributed to the large passivation area of the microelectrodes.

3.3. Cytokines detection by EIS measurements

Electrochemical impedance spectroscopy (EIS) is a very powerful tool for the characterization of surface interfaces and for the detection of very small changes occurring at biosensors surface. EIS is widely used in electrochemical biosensing both as a read-out for analyte binding and as a confirmatory technique to validate the immobilization of biomaterials upon a sensors surface.

Here, an important stage in developing the impedimetric technique was to; first, optimize the polarization potential. A series of measurements were carried out at potentials ranging from 0.3 to −0.3 V in order to establish the optimum value. An applied potential of 0.228 V led to a semi-circular Nyquist plot for the functionalized gold microelectrodes with CMA-modified anti-IL-10. The impedance spectra showed a good stability at 0.228 V and this potential was used for all EIS measurements.

We next studied the performance and sensitivity of the biosensor platform based on the integrated microelectrode modified with CMA-mAb-IL-10 and CMA-mAb-IL-1b for the detection of antigens IL-10 and IL-1b by performing EIS measurements, respectively. After antibodies immobilization onto the WEs, the EIS measurements were performed for all WEs in solution of 5 mM of $K_3[Fe(CN)_6]/K_4[Fe(CN)_6]$ in PBS buffer at pH 7.4. The EIS data from a representative biosensor platform are presented as Nyquist plots in Fig. 5(I) and (II) for different concentrations of IL-10 and IL-1b, respectively. The

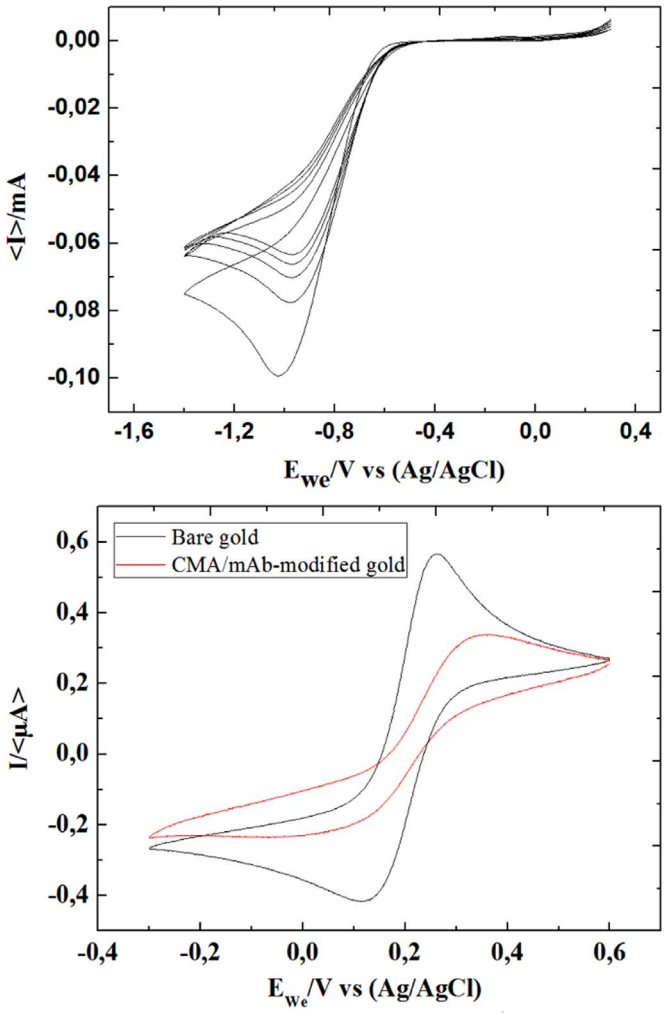

Fig. 4. Cyclic voltammograms of (I) CMA-modified anti-IL-10 (20 mg mL^{-1}) in 5 mM HCl solution. Potential scanned from 0.3 V to −1.4 V vs Ag/AgCl RE. Five cycles performed at a scan rate of 0.1 V/s. (II) CV of: (black) bare gold and (red) after CMA-mAb deposition.

first Nyquist plot semi-circle corresponds to the immobilized antibodies anti-IL-10 and anti-IL-1, respectively. Afterwards, the biosensor platform was rinsed abundantly with PBS in order to prevent denaturation of the antibodies and to remove all adsorbed electrolyte solution from the sensitive layer. Immediately afterwards, the biosensor platform was incubated in a solution containing 1 pg mL^{-1} of IL-10 and 1 pg mL^{-1} of IL-1 for 30 min at 4 °C. After the incubation step, the biosensor platform was once again washed abundantly with PBS in order to remove all unbounded cytokines and placed within the electrolyte solution for EIS measurements. Here, the second Nyquist plot semi-circle (of both IL-10 and IL-1) has increased from the first showing the biorecognition phenomenon of each antibody with their corresponding cytokine. A significant increase in impedance was observed with increasing IL-10 and IL-1b concentration, as evidenced by the increasing diameter of the semi-circular Nyquist traces.

The Nyquist plot semi-circles were fitted using the Randles equivalent circuit model (Fig. 5II inset), where: R_s (solution resistance), R_{ct} (charge-transfer resistance), W (Warburg impedance), and Q1 (constant phase element, an equivalent model of double-layer capacitance) (Baraket et al., 2011). The normalized data were presented as $\Delta R_{ct}/R_{ct}$ (where $\Delta R_{ct}= R_{ct}^{(cytokines)}- R_{ct}^{(antibodies)}/R_{ct}^{(antibodies)}$) as a function of IL-10 and IL-1b concentration, respectively. This is shown in Fig. 6I and II. A linear relationship was found for both cases within the range 1–15 pg mL^{-1} (y=0.64X +0.41, R^2=0.9 for IL-10 and for IL-1b y=0.03X +0.93, R^2=0.93). The limit of

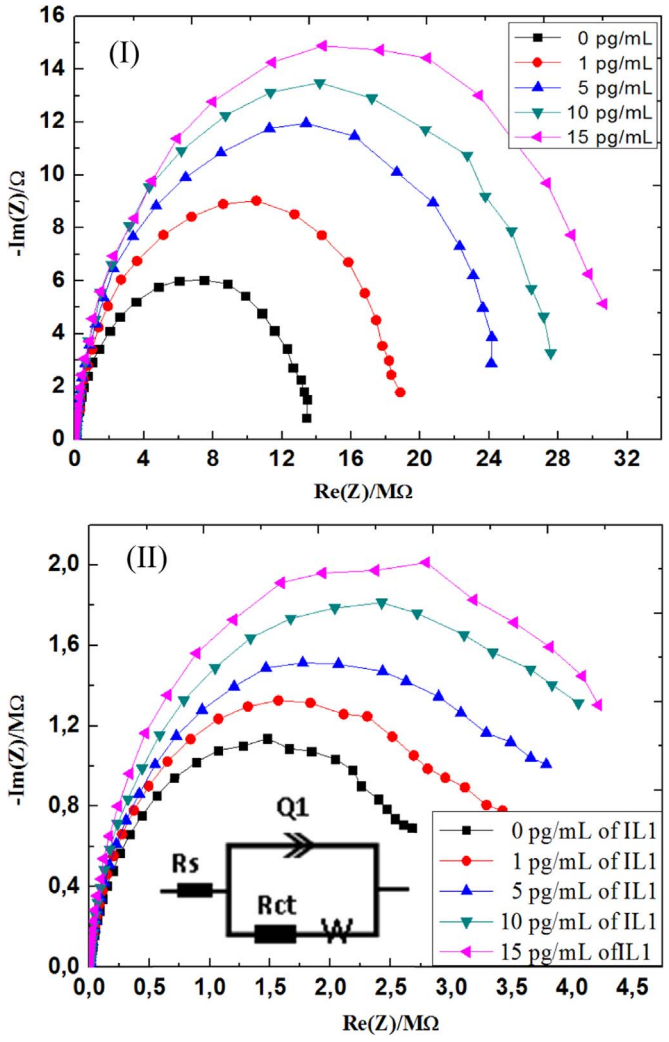

Fig. 5. Nyquist plots for the impediametric detection of (I) human IL-10 and (II) human IL-1.

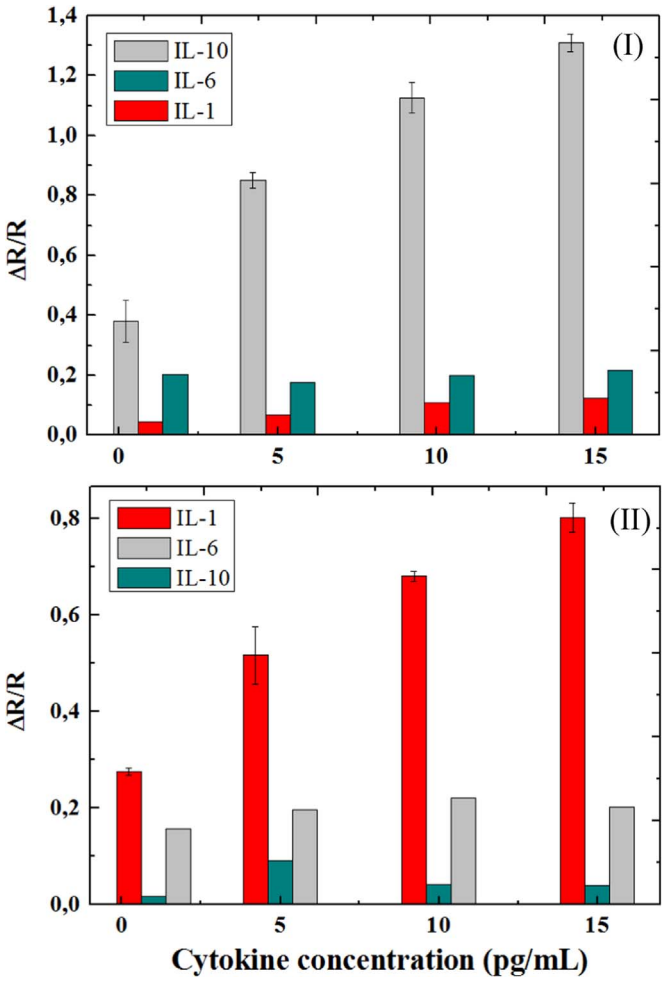

Fig. 6. Normalization of the EIS measurements on modified gold microelectrodes for the detection of (I) human IL-10 and (II) IL-1b with interferences ranging from a concentration of 1 pg mL^{-1} to 15 pg mL^{-1}.

detection (LOD) of the biosensor was 0.3 pg mL^{-1} and 0.7 pg mL^{-1} for IL-10 and IL-1b respectively. This was calculated using the equation 3xStd/slope with Std being the standard deviation.

In our previous study for cytokines detection (Baraket et al., 2014), we applied only one WE using an external RE and CE. The incubation time of each concentration was 30 min, while the analysis with washing, filling the electrolyte solution in the cell, and the experimental setting was around 15 min which gives a total of 45 min for each concentration. This method was repeated for 4 concentrations which gave a total time of 3 h. This was only for the detection of cytokines without accounting the time of preparation of the biosensor surface (immobilization of antibodies). All this time is only for one gold WE. This means that a study of reproducibility will require a repeat all these steps for at least 3 or 5 times.

However, in the present biosensor platform, only one analysis can provide eight sets of data using the eight gold WEs. Moreover, we have spent only one time to biofunctionalize all gold WEs. This means that in a maximum of 5 h we can obtain all data with reproducibility of the measurements.

3.4. Cytokines selectivity and sensitivity measurements

In order to study the selectivity, CMA-mAb anti-IL-10 and CMA-mAb anti-IL-1b were immobilized separately onto another new biosensor platform. Therefore, after CMA-mAb-IL-10 immobilization, the biosensor platform was incubated this time in solutions with increased concentrations of IL-6 and IL-1b, respectively. This applied the same procedure used previously for the detection process. Following EIS measurements and after normalization of R_{ct}; the sensitivity of the biosensor platform towards the IL-10 cytokine was clearly higher when compared to the interferences of IL-6 and IL-1b (Fig. 6(I)). This means that the WE that corresponds to mAb-IL-10 was more sensitive and selective for the IL-10 cytokine.

The same behavior of selectivity was seen for IL-1b detection (Fig. 6(II)) using another WE of the biosensor platform modified with CMA-mAb-IL-1b. The WE that corresponded to mAb-IL-1b was more sensitive and selective for IL-1b cytokine. All these EIS results indicate that the interaction between the cytokines (IL-1b and IL-10) and their corresponding mAb's (mAb-IL-10 and mAb-IL-1b) highlight the possibility of multiplex detection of these biomarkers in the same biosensor platform.

4. Conclusion

In the present work, we have demonstrated the possibility of multiplex detection of biomarkers present in the inflammation areas after LVAD implantation using a fully integrated biosensor platform. IL-1 and IL-10 cytokines were detected within the range of 1–15 pg mL^{-1} which is the critical range in the case of inflammation. The corresponding antibodies of these biomarkers were electroadressed onto the WE's and cytokines were quantified using EIS measurements. The selectivity and the sensitivity of the biosensor

platform were clearly higher towards the corresponding cytokine when compared to other interferences which may be present in the inflammatory area. This opens up the possibility to detect different pro- or anti-inflammatory cytokines by using several WE's. An important decrease of the analysis time can be reached by using this biosensor platform since it was possible to conduct multiple EIS measurements to detect several cytokines at the same time. This will be very helpful to provide data to doctors and clinicians only a few hours after LVAD implantation.

Acknowledgments

This work was funded by the European Communities Seventh Framework Programme (FP7/2007–2013) under the grant agreement No. 248763 (SensorART-IP). We acknowledge the funding through the European Communities Seventh Framework Programme entitled Sea-on-a-Chip (FP7-OCEAN-2013) (No. 614168) and funding from the European Union's Horizon 2020 Research and Innovation Programme entitled HEARTEN under grant agreement No 643694″ and µMole grant agreement No 643694 and No 653626 respectively.

References

Corgier, B.P., Marquette, C.A., Blum, L.J., 2005. J. Am. Chem. Soc. 127, 18328–18332.
Baraket, A., Lee, M., Zine, N., Besseuille, F., Yaakoubi, N., Trivella, M.G., Bausells, J., Zabala, M., Jaffrezic-Renault, N., Errachid, A., 2011. Int. J. Artif. Organs 34, 661–662.
Baraket, A., Lee, M., Zine, N., Sigaud, M., Yaakoubi, N., Trivella, M.G., Zabala, M., Bausells, J., Jaffrezic-Renault, N., Errachid, A., 2013. Sens. Actuators B: Chem. 189, 165–172.
Baraket, A., Lee, M., Zine, N., Yaakoubi, N., Bausells, J., Errachid, A., 2016. Microchim. Acta 183 (7), 2155–2162.
Baraket, A., Lee, M., Zine, N., Yaakoubi, N., Giovanna Trivella, M., Elaissari, A., Sigaud, M., Jaffrezic-renault, N., Errachid, A., 2014. Sens. Transducers 27, 15–21.
Benlarbi, M., Blum, L.J., Marquette, C.A., 2012. Biosens. Bioelectron. 38 (1), 220–225.
Caruso, R., Trunfio, S., Milazzo, F., Campolo, J., Maria, R.D., Colombo, T., Parolini, M., Cannata, A., Russo, C., Paino, R., Frigerio, M., Martinelli, L., Parodi, O., 2010. Am. Soc. Artif. Intern. Organs 56, 313–318.
Chebil, S., Hafaiedh, I., Sauriat-Dorizon, H., Jaffrezic-Renault, N., Errachid, A., Ali, Z., Korri-Youssoufi, H., 2010. Biosens. Bioelectron. 26 (2), 736–742.
Corgier, B.P., Marquette, C.A., Blum, Lc.J., 2007. Biosens. Bioelectron. 22 (7), 1522–1526.
Dorothee, G., Robert, M., Janos, V., Erik, R., 2008. Sens. Actuators B: Chem. 3 (8), 1400–1458.
Gullestad, L., Ueland, T., Vinge, L.E., Finsen, A., Yndestad, A., Aukrust, P., 2012. Cardiology 122 (1), 23–35.
Hou, Y., Helali, S., Zhang, A., Jaffrezic-Renault, N., Martelet, C., Minic, J., Gorojankina, T., Persuy, M.-A., Pajot-Augy, E., Salesse, R., Bessueille, F., Samitier, J., Errachid, A., Akimov, V., Reggiani, L., Pennetta, C., Alfinito, E., 2006. Biosens. Bioelectron. 21 (7), 1393–1402.
Kaptoge, S., Seshasai, S.R.K., Gao, P., Freitag, D.F., Butterworth, A.S., Borglykke, A., Di Angelantonio, E., Gudnason, V., Rumley, A., Lowe, G.D.O., JÃ¸rgensen, T., Danesh, J., 2014. Eur. Heart J. 35 (9), 578–589.
Kongsuphol, P., Ng, H.H., Pursey, J.P., Arya, S.K., Wong, C.C., Stulz, E., Park, M.K., 2014. Biosens. Bioelectron. 61 (0), 274–279.
Lee, M., Zine, N., Baraket, A., Zabala, M., Campabadal, F., Sigaud, M., Caruso, R., Trivella, M.G., Jaffrezic-Renault, N., Errachid, A., 2012. Sens. Actuators B 175, 201–207.
Mazher-Iqbal, M., Desmulliez, M.P.Y., 2011. Lab Chip 11 (4), 569–595.
Navarri, R., Lunghetti, S., Cameli, M., Mondillo, S., Favilli, R., Scarpini, F., Puccetti, L., 2015. Int. J. Cardiol. Heart Vasc. 7, 153–157.
Nymo, S.H., Hulthe, J., Ueland, T., McMurray, J., Wikstrand, J., Askevold, E.T., Yndestad, A., Gullestad, L., Aukrust, P., 2014. Eur. J. Heart Fail. 16 (1), 168–175.
Polsky, R., Harper, J.C., Wheeler, D.R., Dirk, S.M., Arango, D.C., Brozik, S.M., 2008. Biosens. Bioelectron. 23 (6), 757–764.
Prats-Alfonso, E., GarcÃa-MartÃn, F., Bayo, N., Cruz, L.J., Pla-Roca, M., Samitier, J., Errachid, A., Albericio, F., 2006. Tetrahedron 62 (29), 6876–6881.
Pui, T.-S., Agarwal, A., Ye, F., Huang, Y., Chen, P., 2011. Biosens. Bioelectron. 26 (5), 2746–2750.
Qureshi, A., Gurbuz, Y., Niazi, J.H., 2012. Sens. Actuators B: Chem. 171–172, 62–76.
Rohde, L.E., Bertoldi, E.G., Goldraich, L., Polanczyk, C.A., 2013. Nat. Rev. Cardiol. 10 (6), 338–354.
Slaughter, M.S., Pagani, F.D., Rogers, J.G., Miller, L.W., Sun, B., Russell, S.D., Starling, R.C., Chen, L., Boyle, A.J., Chillcott, S., Adamson, R.M., Blood, M.S., Camacho, M.T., Idrissi, K.A., Petty, M., Sobieski, M., Wright, S., Myers, T.J., Farrar, D.J., 2010. J. Heart Lung Transplant. 4 (4), S1–S39.
Soman, G., Yang, X., Jiang, H., Giardina, S., Mitra, G., 2011. J. Immunol. Methods 373 (1–2), 181–191.
Stumpf, C., Lehner, C., Yilmaz, A., Daniel, W.G., Garlichs, C.D., 2003. Clin. Sci. 105, 45–50.